FIBRES & TEXTILES in Eastern Europe

FIBRES & TEXTILES in Eastern Europe

Review • DOI: 10.2478/ftee-2026-0012 • FTEE • 34(1) • 2026 • 110–129

Carbonised Fibre-based Materials For Water Purification And Industrial Wastewater Treatment: A Review Of Textile-derived Filtration Systems

Marcin Henryk Kudzin*, Magdalena Olak-Kucharczyk, Zdzisława Mrozińska, Martyna Gloc, Monika Sikora, Iwona Kucińska-Król, Joanna Olczyk, Anetta Walawska, Renata Żyłła

Łukasiewicz Research Network – Łódź Institute of Technology, ul. Marii Skłodowskiej-Curie 19/27, 90-570 Łódź, Poland
**Corresponding author. E-mail: marcin.kudzin@lit.lukasiewicz.gov.pl*

Abstract
Carbonised fibres derived from polyacrylonitrile fibres, cellulose fibres, chitosan fibres, and lignin fibres, as well as from textile waste, have emerged as promising materials for industrial wastewater treatment. Their performance depends on precursor type, carbonization conditions, and activation, which determine the pore structure and surface chemistry. This review summarizes recent advances in the production and functionalization of carbonised fibre-based adsorbents, including oxidation, polymer grafting, nanoparticle incorporation, and nitrogen doping. Particular attention is given to textile-derived nonwoven structures used for the removal of heavy metals, dyes, aromatic amines, pharmaceuticals, and microplastics. Challenges related to regeneration, fouling, industrial implementation, and circular-economy applications are also discussed.

Keywords
Activated carbon fibre, Carbonized fibres, Heavy metal removal, Surface functionalization, Textile wastewater treatment

1. Introduction

Access to clean water is under increasing pressure globally. UN estimates put the number of people living in high water-stress regions at over two billion, with supply deficits projected to deepen in many areas by 2050 [1]. Industrial consumption contributes substantially to this pressure and tends to receive less policy attention than agriculture. In Poland, industry accounts for more than 70% of total annual freshwater withdrawals – roughly 7 billion cubic metres, a figure dominated by cooling-water abstraction in the energy sector – drawing from river basins that also supply drinking water to urban populations [2].

The textile sector is a disproportionate contributor. Wet-processing operations – scouring, bleaching, dyeing, printing, and finishing – require water as a reaction medium for salts, alkalis, acids, surfactants, and process chemicals across a wide pH range [3,4]. Processing 1 kg of dyed cotton generates approximately 100–150 litres of effluent [5], and the industry is estimated to contribute substantially to industrial water pollution globally, with some reports suggesting a share of up to 20% [6], though this figure draws on grey literature and should be treated with caution – discharging dyes, aromatic amines, heavy metals, phthalates, and volatile organic compounds into receiving waters. Aromatic amines warrant particular attention: they form through reductive cleavage of azo dye bonds under environmental or metabolic conditions, many are classified as confirmed or suspected carcinogens under EU REACH Annex XVII [7], and their presence in surface waters linked to textile processing and laundering has been documented, though contamination data remain fragmentary and geographically uneven; an early report of river contamination by aromatic amines from azo-dye cleavage [8] predates the tightening of REACH restrictions and substantial changes in the textile sector's use of these substances since then [9].

Conventional treatment based on activated sludge is effective for readily biodegradable organic load, but handles recalcitrant dyes, heavy metals, and persistent micropollutants such as pharmaceuticals and microplastics poorly [10]. More advanced options – chemical precipitation, coagulation–flocculation, adsorption on granular activated carbon, and membrane filtration – are technically capable of addressing these contaminants, but their cost and operational complexity represent a significant barrier for small- and medium-sized enterprises, which make up the majority of textile processors in Poland and in much of Central Europe. The result is that investment in wastewater upgrading remains low despite tightening regulatory requirements, and there is practical demand for treatment materials that offer high performance at manageable cost and can be regenerated on-site [11].

Carbon-based adsorbents – activated carbons, carbon nanotubes, graphene oxide, biochar – have received sustained research attention for water treatment [12,13]. High surface area and chemically versatile surfaces are the main reasons. Among these, carbonised fibre-based materials obtained from textile precursors have certain practical advantages. Controlled carbonisation of fibrous starting materials preserves the original fabric architecture, producing three-dimensional porous networks that combine activated-carbon-type adsorption capacity with the mechanical integrity and formability of woven or nonwoven textiles [14,15]. This makes it possible to fabricate structured filter elements – rather than loose granular beds – that can sustain continuous flow-through operation without significant pressure

Open Access. © 2026 Marcin Henryk Kudzin *et al.*, published by Łukasiewicz Research Network, Institute of Biopolymers and Chemical Fibres. This work is licensed under the Creative Commons Attribution-NonCommercial-NoDerivs 4.0 License.

drop or channelling, which is relevant for multi-stage cascade configurations.

The fibre precursors studied to date include polyacrylonitrile fibres (PAN), cellulose fibres and their derivatives, chitosan fibres, lignin fibres, and various lignocellulosic waste materials. PAN is the most extensively investigated, drawing on the well-established stabilisation and carbonisation knowledge accumulated in the carbon-fibre composite industry [16,17]. Cellulose fibre-derived carbons are of interest as renewable bio-based alternatives, and the oxygen-rich surface groups they carry after moderate-temperature carbonisation facilitate further chemical modification [18]. Chitosan, obtained from crustacean chitin by alkaline deacetylation, introduces dense primary amine groups onto the carbon surface; after pyrolysis, these are converted into pyridinic-N, pyrrolic-N, and graphitic-N species, which may contribute to enhanced affinity for transition-metal ions such as Cu^{2+}, Pb^{2+}, and Cd^{2+} depending on the retained nitrogen configuration [19]. Combining biopolymer and synthetic fibre precursors – by blending or co-spinning – gives further scope for adjusting the adsorption characteristics and mechanical properties of the final filter element [20].

Multi-stage or cascade filtration, in which several filter stages with different functions are arranged in series, offers a practical way to deal with the complex composition of textile effluents [10]. A coarse stage can remove suspended solids and microfibres; intermediate stages with functionalised activated-carbon nonwovens adsorb heavy metals and dyes; a final polishing stage targets trace organics and residual colour. When preceded by advanced oxidation (ozonation, UV/H_2O_2, *Fenton* chemistry, or persulfate activation) and followed by nanofiltration or reverse osmosis, such trains can produce effluent of sufficient quality for reuse in the dyehouse or finishing bath [21]. Integrated advanced oxidation process (AOP)-membrane configurations remain comparatively underexplored relative to their individual components, with process design, fouling control, and energy demand identified as the main barriers to wider adoption [21]. Recent pilot-scale work combining nanofiltration, reverse osmosis, and persulfate oxidation of biologically treated textile effluent has reported permeate specific energy consumption as low as 0.38–1.2 kWh m^{-3}, with nanofiltration at moderate pressure identified as the most energy-efficient configuration [22]. The economic incentive to close the water loop within the production facility, reducing both freshwater intake and wastewater discharge fees, makes this approach attractive even for small- and medium-sized enterprises, particularly in regions where freshwater abstraction and discharge charges are rising. Closed-loop and zero-liquid-discharge approaches specifically for the textile sector have advanced substantially since 2020, driven by tightening discharge regulations and rising freshwater costs [23].

Existing reviews usually focus on individual aspects of carbonised fibre materials, whereas comprehensive coverage of precursor selection, carbonisation, functionalisation, pollutant removal, and practical applications remains scarce. This review provides an integrated overview of textile-derived carbonised fibres, covering precursor materials, carbonisation and activation processes, surface modification strategies, pollutant removal mechanisms, and the application of carbonised nonwovens in cascade filtration systems. Particular attention is given to regeneration, scale-up challenges, and the circular use of post-consumer textile waste as a feedstock for advanced filtration materials.

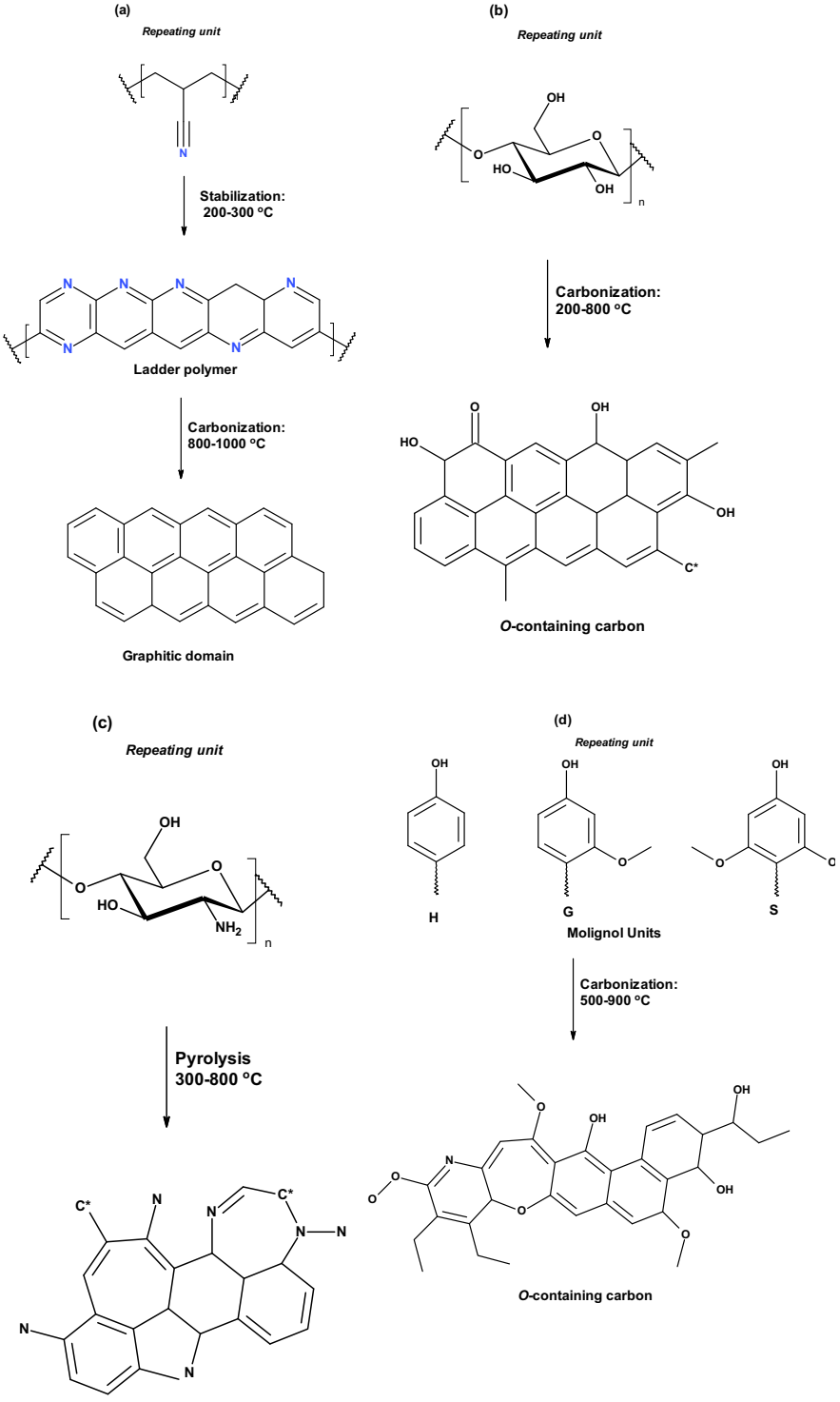
2. Textile-Derived Precursors and Carbonisation

Precursor choice shapes carbon yield, pore development, surface chemistry, and ultimately the adsorption performance of the resulting fibres. The main precursor groups studied to date are discussed below, with attention to how each affects properties relevant to water-treatment use. Figure 1 summarizes the principal textile-derived carbon precursors and their transformation pathways during stabilisation, pyrolysis, and carbonisation. The resulting surface chemistry – oxygen groups in CEL-derived carbons, nitrogen configurations in Cts-derived carbons, and graphitic domains in PAN- and LIG-derived carbons – directly governs contaminant selectivity in the filtration systems described in Section 4 [16,24–28].

2.1 Polyacrylonitrile Fibres

PAN has been used as a carbon-fibre precursor since the 1960s, and the processing knowledge accumulated in the structural-composites sector applies largely unchanged to activated carbon fibre (ACF) manufacture for water treatment. Fibres are produced by wet or dry-jet wet spinning from acrylonitrile homo- or copolymers – small additions of itaconic acid or methyl acrylate moderate the exothermic cyclisation during stabilisation [24]. Heating in air at 200–300°C converts the nitrile groups into a thermally stable ladder structure of conjugated C–N and C–C bonds, after which the fibre can withstand the subsequent high-temperature step [25]. Carbonisation in nitrogen or argon at 800–1600°C removes most heteroatoms and leaves a turbostratic graphitic matrix with carbon content above 92 wt% [16]. Carbon yield is 50–55%, markedly higher than for most natural precursors, and partly compensates for the higher raw-material cost.

After activation, PAN-derived ACFs reach Brunauer–Emmett–Teller (BET) surface areas of 1000–2500 $m^2\ g^{-1}$, with well-developed microporosity (pore width < 2 nm) that accounts for their high uptake of small organic molecules [14,29]. When the precursor is in nonwoven form, the bonded fibre architecture survives carbonisation, yielding an activated carbon nonwoven with a defined three-dimensional structure suitable for use in flow-through filter modules [30]. Basis weight, fibre diameter, and inter-fibre void volume are all adjustable in the precursor fabric, providing structural control over the finished filter that granular carbon beds cannot easily match. This tunability is the main practical justification for nonwoven PAN-ACF in cascade filter designs.



(a) PAN: stabilization (200-300 °C) then carbonization → graphitic carbon domains. (b) CEL: carbonization → oxygen-containing carbon. (c) Cts: pyrolysis → nitrogen-doped (pyridinic-/pyrrolic-/graphitic-N) carbon. (d) LIG: carbonization → highly aromatic, higher-yield carbon.

Figure 1. Main chemical structures of representative textile-derived carbon precursors and their thermal transformation pathways: (a) polyacrylonitrile fibre (PAN), (b) cellulose fibre (CEL), (c) chitosan fibre (Cts), and (d) lignin fibre (LIG) [16,24–28].

2.2 Cellulose Fibres and Their Carbonisation

Carbon fibres from rayon (regenerated cellulose) predate PAN-based fibres commercially, with early applications in aerospace dating to the 1950s [16]. Viscose, lyocell, and natural cotton have all been carbonised to produce porous carbon materials for environmental applications. The practical drawback versus PAN is low carbon yield: pyrolysis of cellulose fibres typically delivers only 20–30 wt% carbon because competing depolymerisation and dehydration reactions convert much of the mass to volatiles [30]. Pretreating with phosphoric acid or zinc chloride, or using a hydrothermal step prior to carbonisation, promotes char formation and can raise yield to 35–45% [26].

Carbonised cellulose fibres retain meaningful amounts of surface oxygen functionality – carboxyl, lactone, and phenol groups – when carbonised at moderate temperatures (below about 900°C). This amphoteric character supports adsorption of cationic metal ions through ion exchange, complexation, and electrostatic attraction, the relative contributions of which shift with pH and the extent of surface oxidation [18]. It should be noted that aerogels cast from cellulose nanofibre or cellulose nanocrystal suspensions are not fibrous in the classical textile-precursor sense – they originate from nanocellulose suspensions rather than spun or natural cellulose fibres – but, after carbonisation, they give very-low-density carbon sponges with open macro- and mesopore networks [31], and are mentioned here only for functional comparison with fibre-based ACF media. This hierarchical porosity supports higher filtration velocities than predominantly microporous PAN-ACFs, which can be useful when high filtration velocity matters more than maximum surface area.

2.3 Chitosan-Based Fibres

Chitosan is obtained from crustacean shells by alkaline deacetylation of chitin. What distinguishes it from PAN fibres or cellulose fibres as a precursor is the high density of primary amine groups ($-NH_2$) along the backbone, which coordinate transition-metal ions through nitrogen lone-pair donation and electrostatic mechanisms. Upon pyrolysis, however, the $-NH_2$ groups are not retained as such; instead, nitrogen is incorporated into pyridinic-N, pyrrolic-N, and graphitic-N configurations. Pyridinic and pyrrolic sites at pore edges retain lone-pair donor character and are responsible for the selective affinity of carbonised chitosan for Cu^{2+}, Pb^{2+}, Hg^{2+}, Cd^{2+}, and Ni^{2+} [32]. The degree of deacetylation, typically 75–95% for commercial grades, controls amine density and hence metal-adsorption capacity [33]. Fibres can be wet-spun from dilute acetic acid solution; crosslinking with glutaraldehyde or epichlorohydrin before pyrolysis improves dimensional stability. Pyrolysis of crosslinked chitosan at 600–900°C under nitrogen yields nitrogen-doped porous carbons with 2–8 at % N, which may enhance electrostatic affinity for anionic species depending on the predominant nitrogen configuration (pyridinic vs. graphitic N) and solution pH, and can improve catalytic activity in oxidative processes [32].

2.4 Lignocellulosic and Waste-Derived Precursors

Flax, hemp, jute, coir, and kenaf have all been tested as ACF precursors. Their heterogeneous cell-wall structure – cellulose microfibrils in a hemicellulose-lignin matrix – tends to give broader and less predictable pore-size distributions than pure cellulose fibres or PAN [27]. Lignin deserves separate mention: available in large quantities from pulp and paper production, it has carbon yields of 40–50 wt % depending on lignin source (kraft, organosolv, or soda) and carbonisation temperature, which are closer to PAN than most polysaccharide precursors [28]. Post-consumer textile waste, mainly cotton-polyester blends, has also been examined as a feedstock. Pyrolysis of such mixed-fibre waste gives composite carbons in which the polyester-derived aromatic carbon structures provide a degree of structural reinforcement and the cellulose-fibre-derived fraction contributes surface functional groups [34]. Feedstock heterogeneity is a real problem for process control and reproducibility, but cost and end-of-life management considerations continue to motivate interest in waste-derived feedstocks. In practice, however, the cotton-to-polyester ratio in post-consumer streams varies widely between garment grades and collection sources, and few studies have evaluated whether carbonisation protocols optimised on model single-fibre textiles transfer reliably to unsorted blends. Reported BET surface areas and adsorption capacities for waste-derived carbons show substantially larger inter-study variability than for PAN or virgin cellulose precursors, and reproducibility within ±20% between batches has rarely been demonstrated [34]. Until robust presorting and blending protocols are established at industrial scale, batch-to-batch consistency remains an unresolved obstacle for waste-textile carbonisation feedstocks.

2.5 Carbonisation and Activation Processes

Whatever the precursor, ACF production follows the same general sequence. An optional pre-treatment step – oxidative stabilisation for PAN, catalyst impregnation for cellulose fibres – prepares the fibre for carbonisation at 600–1600°C in an inert atmosphere, which removes heteroatoms and develops the turbostratic carbon structure. Activation then opens and expands the pore network. Physical activation uses steam or CO_2 at 800–1000°C; the *Boudouard* reaction ($C + CO_2 \rightarrow 2CO$) preferentially burns off the most reactive carbon at defect sites and pore edges, giving predominantly microporous products with narrow pore-size distributions. Chemical activation with KOH – the most widely used agent – works by intercalation and subsequent volatilisation of potassium species, which generates additional mesopores alongside existing micropores; BET areas above 3000 $m^2\ g^{-1}$ have been reported under optimised laboratory conditions, though at this level of porosity mechanical integrity tends to be compromised [35,36].

Precursor	C yield (%)	Surface groups after carbonisation	Advantages	Limitations	Applications in water treatment	Refs
PAN	50–55	Graphitic domains; residual N-containing groups	High carbon yield; good mechanical stability; controllable pore structure	Fossil-derived; higher production cost	Heavy metals, dyes, pharmaceuticals; ACF filter media	[14,16,24,25,30]
Cellulose fibre (cotton, viscose, lyocell)	20–30 (untreated); 35–45 (H_3PO_4/$ZnCl_2$ or hydrothermally pre-treated)	–COOH, –OH, phenolic groups	Renewable; widely available; oxygen-rich surface	Low carbon yield; limited structural stability	Dye adsorption, metal ions; fast-flow filtration	[30,41] (untreated); [26] (pre-treated)
Chitosan fibre	~20 (as-spun); higher with NH_4Cl pre-treatment	Nitrogen functionalities (pyridinic-N, pyrrolic-N, graphitic-N)	High selectivity for metal ions; chelation capacity	Lower thermal stability; relatively high cost	Cu^{2+}, Pb^{2+}, Cd^{2+} removal; catalytic systems	[42]
Lignin fibre	40–50	Aromatic carbon; O-functional groups	Higher yield among biomass precursors; low raw material cost	Variable feedstock composition; batch-to-batch inconsistency	Activated carbons; dye adsorption	[27,28]
Lignocellulosic fibres (flax, hemp, jute)	20–40	Mixed O-containing groups	Waste valorisation potential; low feedstock cost	Variable composition; reproducibility issues	Bio-based adsorbents; filtration media	[27,34]
Textile waste (cotton/polyester blends)	25–45	Mixed graphitic and O-functional groups	Circular economy potential; diverts waste from landfill	Heterogeneous composition; requires pre-sorting	Wastewater treatment; hybrid adsorbents	[34]

Table 1. Comparative characteristics of major textile-derived precursors for carbonised fibre production.

Temperature is the variable with the most pronounced effect on pore structure and surface chemistry. Below about 700°C, a significant share of heteroatom functionality is retained – oxygen and nitrogen groups useful for adsorbing polar contaminants but that limit graphitic order and electrical conductivity. Above 1200°C, graphitic ordering increases, which strengthens π–π stacking interactions with aromatic pollutants but reduces the density of ion-exchange-active surface groups [37]. For water-treatment purposes, 800–1000°C followed by mild activation is generally where the useful range lies: BET areas fall between 800 and 1500 m^2 g^{-1}, the pore structure is mixed micro-mesoporous, and enough residual oxygen functionality survives to maintain wettability and ion-exchange capacity. Heating rate and hold time at peak temperature have secondary but measurable effects: slow ramp rates (1–3°C min^{-1}) promote more uniform pore development, whereas rapid pyrolysis can create gaseous-product concentration gradients that cause cracking along the fibre cross-section [38].

For filter module applications, the dimensional changes that occur during carbonisation require attention. PAN nonwovens typically shrink 20–40% linearly depending on stabilisation conditions, applied tension, and precursor composition, and the shrinkage is anisotropic – more pronounced along the fibre length than across the cross-section – which can distort a module fabricated to defined dimensions [39]. Pre-tensioning the precursor fabric during the thermal treatment and optimising the heating profile can keep planar distortion below about 5%, sufficient to preserve inter-fibre pore geometry and ensure predictable pressure drop across the filter element.

PAN remains the most widely used starting material for high-performance ACFs, though bio-based and waste-derived alternatives have attracted growing interest as routes to more sustainable production [40]. The main precursor groups are compared in Table 1.

3. Surface Functionalisation Strategies

As-carbonised PAN and cellulose fibres carry a hydrophobic, weakly acidic surface [43]. This is suitable for non-polar organics and positively charged dyes, but not for the selective removal of anionic species or specific heavy-metal ions. Without modification, carbonised fibre filters work for a limited contaminant range. Surface functionalisation is what extends them to the full spectrum of industrial effluent chemistry.

The most widely applied approaches involve oxidative activation of carbon surfaces and the introduction of amine-containing functionalities through polymer grafting. These modifications increase surface polarity, improve wettability, and create adsorption-active sites capable of interacting with metal ions, dyes, and other polar contaminants. Representative pathways of oxidative functionalisation and polyethylenimine (PEI) grafting are schematically illustrated in Figure 2.

3.1 Physicochemical Characterisation of Carbonised Fibre Surfaces

Interpreting adsorption data and comparing results across studies requires consistent characterisation of both surface chemistry and pore structure. X-ray photoelectron spectroscopy (XPS) is the primary tool for quantifying surface elemental composition and for resolving the chemical state of heteroatoms: deconvolution of the N 1 s core-level spectrum distinguishes pyridinic-N (~398.5 eV), pyrrolic-N (~400.1 eV), graphitic-N (~401.2 eV), and oxidised-N (~402–405 eV), each of which has a distinct role in metal-ion coordination, electrostatic interactions, and Fenton-type catalysis [43,46]. Raman spectroscopy provides complementary information on graphitic order through the D/G band intensity ratio: the D band (~1350 cm^{-1}) reflects defect-induced disorder at pore edges and grain boundaries, while the G band (~1580 cm^{-1}) corresponds to in-plane vibrations of sp^2-hybridised carbon [47,48]. A high D/G ratio indicates a defect-rich surface with greater density of adsorption-active edge sites; a low D/G ratio reflects more ordered graphitic domains with stronger π–π stacking capacity towards aromatic pollutants. [47,48] Fourier-transform infrared spectroscopy (FTIR-ATR) provides semi-quantitative identification of surface functional groups: carboxyl (~1710–1730 cm^{-1}), conjugated carbonyl (~1600–1650 cm^{-1}),

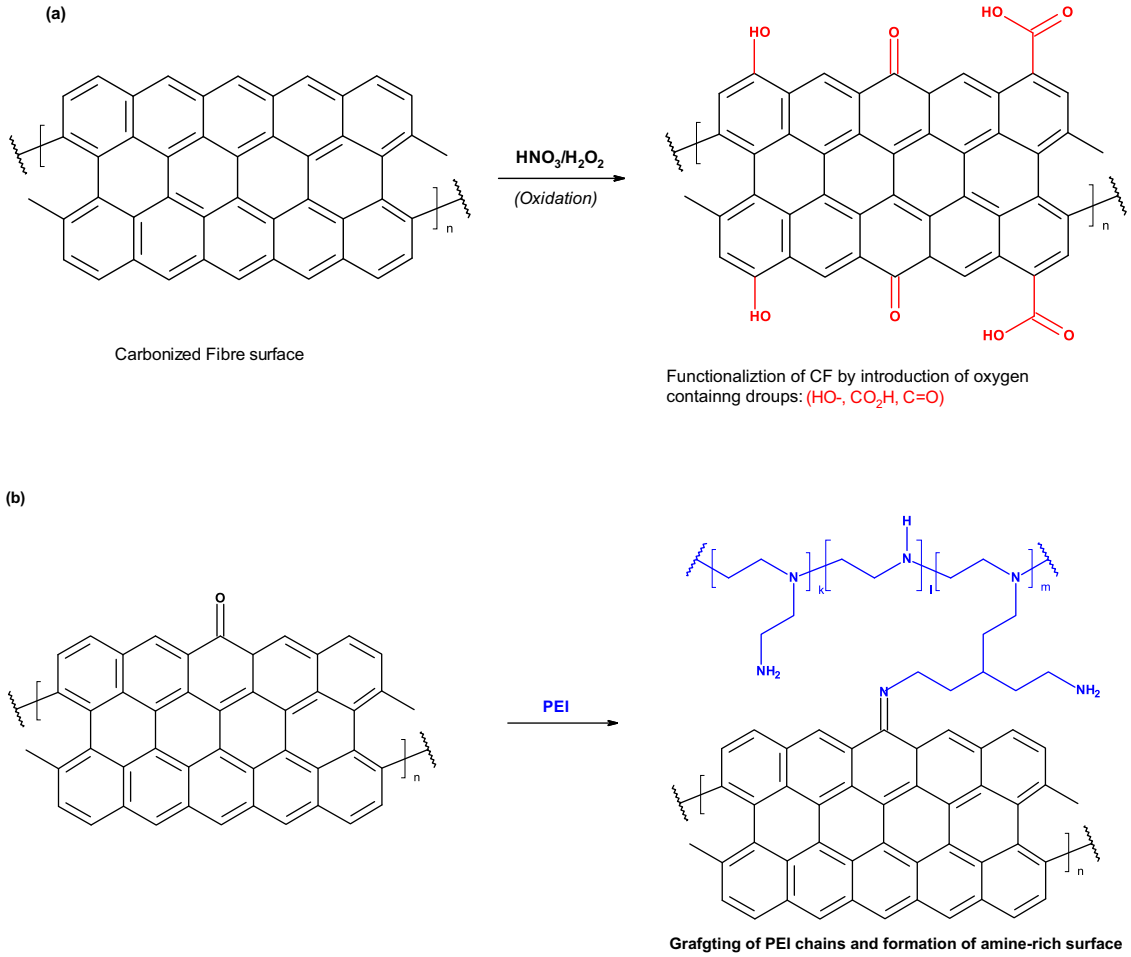


Figure 2. Simplified representative pathways for surface functionalisation of carbonised fibres: (A) oxidative functionalisation introducing oxygen-containing surface groups (-COOH, -OH, C = O) and (B) grafting of PEI chains leading to formation of amine-rich adsorption-active surfaces [44,45].

hydroxyl (broad, 3200–3500 cm^{-1}), and amine N-H stretching and bending bands (3300–3500 and 1550–1650 cm^{-1}, respectively) [44]. Temperature-programmed desorption (TPD) under inert gas provides quantitative data on the density and thermal stability of individual oxygen-containing groups: carboxylic acids release CO_2 at 200–300°C, lactones and anhydrides at 350–600°C, and phenol and carbonyl groups at higher temperatures, though these ranges overlap in practice and peak assignments should be treated as indicative [44]. Pore structure is characterised by N_2 physisorption at 77 K, with the BET equation applied to the multilayer range and non-local density functional theory (NLDFT) used for micropore size distribution analysis; pore widths below 2 nm make a dominant contribution to adsorption capacity for small organic molecules and metal ions [46]. Mercury intrusion porosimetry extends the accessible range into the macropore region (0.1–10 µm) that governs hydraulic permeability and pressure drop in filter modules [49].

These characterisation methods and the parameters they provide are summarised in Table 2.

3.2 Functionalisation Methods

3.2.1 Oxidative Functionalisation

Wet oxidation with HNO_3, H_2O_2, or $(NH_4)_2S_2O_8$, or gas-phase treatment with ozone or air at 300–400°C, introduces carboxyl, carbonyl, lactone, and hydroxyl groups at basal-plane edges and defect sites without large losses of BET surface area [44]. The pH_pzc typically shifts from around 6 on as-carbonised fibres to 4 after HNO_3 oxidation, broadening the pH range over which cationic metal ions are taken up by ion exchange, and improving wettability for filter modules that need rapid wet-out during start-up [50]. Degree of oxidation needs to be controlled: excessive treatment degrades the graphitic structure and reduces micropore volume, so there is a practical ceiling that depends on the intended application [44].

3.2.2 Polymer and Biopolymer Grafting

Polymer grafting places more functional groups on the surface than oxidative etching can achieve and allows more targeted chemical design. PEI, a branched polyamine with primary, secondary, and tertiary amine groups, can be grafted onto oxidised ACFs by carbodiimide-mediated amide coupling; the resulting materials show substantially higher heavy-metal and CO_2 uptake than the unmodified substrate [51]. Chitosan coatings – applied by dip-coating ACF fabrics in dilute acetic acid solution and crosslinking with glutaraldehyde – bring the metal-chelating selectivity of the biopolymer to the filter medium while retaining the mechanical support of the carbon fibre scaffold; Cu^{2+} electrosorption capacity was about 2.2-fold higher on the chitosan-impregnated composite than on the pristine fibre [52]. Coating stability during acid-wash or oxidative regeneration is a persistent practical concern, covalent grafting strategies that resist hydrolytic detachment are therefore under active investigation.

3.2.3 Metal-oxide and Nanoparticle Deposition

Depositing metal-oxide nanoparticles on carbonised fibre surfaces adds photocatalytic or Fenton-type oxidation capability alongside adsorption. TiO_2 anchored by sol-gel or hydrothermal routes [53] generates OH and O_2- under UV irradiation that can mineralise adsorbed dye molecules and thereby regenerate adsorption capacity without added reagents [54]. Fe_3O_4-decorated fibres catalyse heterogeneous Fenton reactions ($Fe^{2+} + H_2O_2 \rightarrow \cdot OH$) in the dark, and their magnetic character simplifies separation in powdered-fibre configurations [55]. Silver and copper nanoparticles at 0.5–2 wt% suppress biofilm formation through sustained ion release and intracellular oxidative stress, which helps in biological prefilter stages where microbial colonisation would otherwise shorten service life [56]. The ecotoxicity of released Ag^+ ions to aquatic organisms is a recognised concern that warrants consideration when Ag-bearing filter stages are deployed in effluent treatment systems. [57] Particle size (ideally below 10 nm), loading, and surface distribution all need to be controlled since aggregates reduce catalytic activity and loose particles can enter the treated water.

Technique	Parameter measured	Typical values	Refs.
XPS (N 1 s deconvolution)	Pyridinic-N, pyrrolic-N, graphitic-N, oxidised-N	~398.5, ~400.1, ~401.2, ~402–405 eV	[43,46]
Raman spectroscopy	D-band/G-band intensity ratio	D ~1350 cm^{-1}; G ~1580 cm^{-1}	[47,48]
FTIR-ATR	Surface functional groups	Carboxyl ~1710–1730; carbonyl ~1600–1650; hydroxyl 3200–3500 (broad); amine N-H 3300–3500 and 1550–1650 cm^{-1}	[44]
TPD (inert gas)	Desorption temperature of O-groups	Carboxylic acids 200–300°C; lactones/anhydrides 350–600°C; phenol/carbonyl at higher temperatures	[44]
N_2 physisorption (BET/NLDFT)	Surface area, micropore size distribution	Pore widths below 2 nm dominant	[46]
Hg intrusion porosimetry	Macropore volume/distribution	0.1–10 µm	[49]

Table 2. Summary of physicochemical characterisation methods for carbonised fibre surfaces.

3.2.4 Nitrogen Doping

Nitrogen content can be increased beyond what the precursor alone provides either by post-carbonisation treatment in ammonia at 700–900°C, or by incorporating nitrogen-rich molecules (melamine, urea, dicyandiamide) into the spinning formulation before fibre formation [58]. The N atoms are incorporated in pyridinic, pyrrolic, and graphitic configurations; pyridinic and pyrrolic sites at pore edges are the most useful for metal-ion coordination and for catalysing oxygen reduction in Fenton-type systems, while graphitic-N raises electrical conductivity [59]. In materials where N-doping is combined with KOH activation, BET areas above 2000 $m^2\ g^{-1}$ and nitrogen contents of 5–8% have been reported, with demonstrated uptake across metal ions, cationic dyes, and antibiotics [60,61].

4. Removal of Priority Pollutants

How well carbonised fibre materials perform in practice comes down to whether they can reduce contaminant concentrations to levels meeting discharge limits or process-water reuse standards. For the textile sector, the pollutants appearing most consistently in both regulation and published work are heavy metals, dyes and aromatic amines, pharmaceuticals and personal care products (PPCPs), and microplastics.

Table 4 presents a comparative overview of representative removal performance for the major pollutant groups discussed in Sections 4.1–4.4. The following subsections discuss the corresponding adsorption mechanisms, removal efficiencies, and representative adsorption capacities reported for carbonised fibre-based materials.

Figure 3 presents representative contaminants discussed in Sections 4.1–4.3 and serves as a reference for the pollutant classes considered throughout this section.

The principal adsorption mechanisms involved in their uptake by functionalised carbonised fibre materials are summarised in Table 3. In practice, pollutant removal is rarely governed by a single interaction mechanism; instead, adsorption typically results from the combined effects of electrostatic attraction, coordination, hydrogen bonding, π–π interactions, and hydrophobic interactions, whose relative contributions depend on pollutant speciation, surface chemistry, pH, and ionic strength [44,51].

4.1 Heavy Metals

Cu^{2+} Pb^{2+}, Cd^{2+}, Hg^{2+}, Ni^{2+}, and Zn^{2+} enter textile effluents mainly from mordanting baths, metallic dye processes, and finishing chemicals. Their uptake on carbonised fibres involves overlapping contributions from physical adsorption into micropores by van der Waals forces, ion exchange at carboxylate and phenolate surface groups (which becomes increasingly important above pH_pzc), and surface complexation at nitrogen-donor sites on N-doped or chitosan-coated fibres [32]. These relative contributions depend on pH, ionic strength, and the coordination chemistry of each metal. Langmuir q_{max} values for Cu^{2+} on chitosan-coated PAN-ACF nonwovens are around 185 $mg\ g^{-1}$ at pH 5.5, roughly 2.5 times the uncoated ACF value under the same conditions, which is consistent with amine-group chelation as the primary uptake route [32]. For $Pb^{2+}$and Hg^{2+}, which form stable N- and S-donor complexes, functionalised ACF fibres have shown 36-fold higher batch capacities than granular activated carbon at sub-10 mg L^{-1} concentrations [62,71].

The limitation of most published work is that single-solute batch tests dominate the dataset, and competitive effects from real effluent matrices are rarely examined. Ca^{2+} and $Mg^{2+}$from water hardness compete with heavy metals for amine and carboxylate sites, and in synthetic hard water (250 $mg\ L^{-1}$ $CaCO_3$ equivalent) effective capacity can be measurably lower than in deionised water, though the magnitude of this competitive effect is highly system dependent, and reported values vary widely across studies. Introducing higher-affinity groups – thiol (–SH) or imidazole – partially restores selectivity since these form thermodynamically preferred complexes with soft-acid Hg^{2+} and Cd^{2+} over competing Ca^{2+} [71].

4.2 Textile Dyes and Aromatic Amines

Textile effluents carry dyes from several structural classes – reactive, acid, basic, vat, and disperse – which differ enough in charge and molecular size that no single adsorption condition handles all of them well. Cationic dyes such as methylene blue (MB) and crystal violet adsorb readily on 16 oxidised ACF at neutral pH via electrostatic attraction to the negative surface and π–π stacking between the aromatic dye rings and graphitic basal planes [15]. For MB on KOH-activated PAN-ACFs, reported q_{max} values exceed 300 $mg\ g^{-1}$, the combination of high microporosity and a net negative surface charge at pH 7 evidently places these materials among the better-performing carbon adsorbents for this dye class [15]. Anionic reactive dyes are more difficult: sulphonate groups give the molecule a net negative charge, so adsorption on an equally negative ACF surface is electrostatically unfavourable above pH 4. Either pH reduction below pH_pzc, or positive surface charge introduced by PEI grafting or chitosan coating (amino groups protonated below pKa ~ 6.3), is needed for effective uptake [27,72,73].

Many aromatic amines – including 4-aminobiphenyl, benzidine, and 2-naphthylamine – are classified as confirmed or probable human carcinogens under REACH Annex XVII, making their removal from effluent a regulatory requirement. On N-doped ACFs at near-neutral pH, adsorption proceeds mainly through π–π electron donor–acceptor interactions between the amine-bearing aromatic rings and the graphitic surface [43,74]. First-order kinetics with half-lives in the 10–25 min range have been reported for aniline and substituted aromatic amines on 16 oxidised and nitrogen-treated ACFs [43,74]; residual

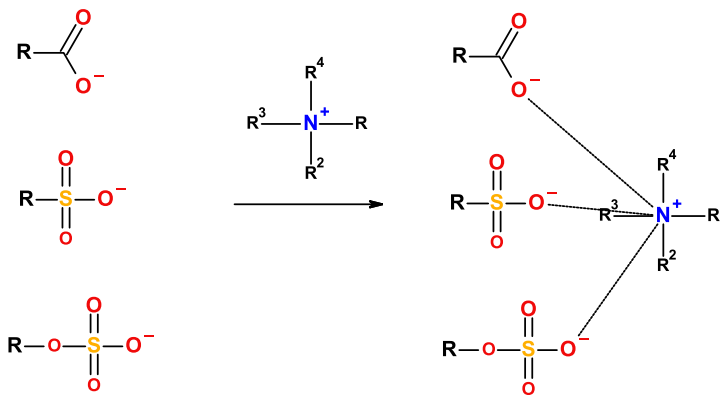
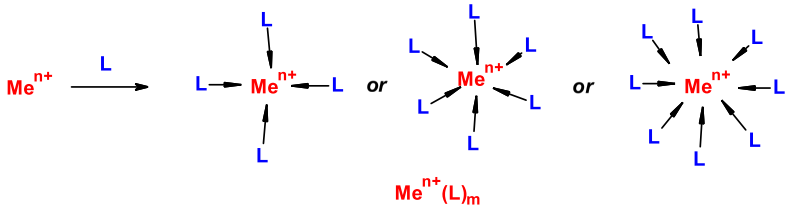
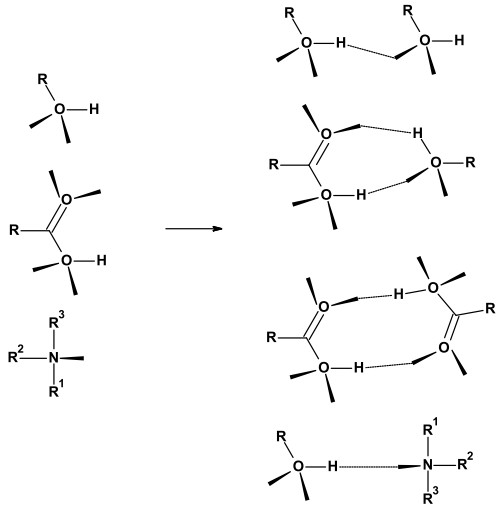
Interaction type	*Scheme*	*Occurrence*	*Ref.*
Electrostatic attraction		**Cationic dyes, protonated amines**	[43,44,70]
Coordination/chelation	 *Coordination number: m = 4, 6, 8; L - neutral ligand or anion*	Heavy metal ions	[51,62,68]
Hydrogen bonding		Pharmaceuticals, amines	[43,69]

Table 3: *Continued*

Interaction type	Scheme	Occurrence	Ref.
π–π Interaction		Aromatic fragments	[43,47,48]
Hydrophobic interaction		Non-polar organic compounds, PAHs, chlorinated solvents, microplastics	[43,51]

The Scheme column presents representative interaction geometries, whereas the occurrence column indicates contaminant classes for which a given mechanism is typically dominant or co-dominant under common aqueous conditions (pH 4–8). In practice, multiple adsorption mechanisms often operate simultaneously, and their relative contributions depend on surface functional group density, pollutant speciation, solution pH, and ionic strength [43,44,47,48,51,64,69,70].

Table 3. Principal adsorption interaction mechanisms between functionalised carbonised fibre surfaces and dissolved pollutants.

concentrations below 0.1 mg L^{-1} are achievable from 50 mg L^{-1} initial solutions, which falls below the EU Water Framework Directive indicative thresholds for priority hazardous substances [7].

4.3 Pharmaceuticals and Personal Care Products

Two entry routes bring PPCPs into textile effluents: wash-off from fibres treated with biocidal or UV-protective finishes, and co-discharge with municipal wastewater at shared treatment sites. Tetracycline antibiotics, present in surface waters at 0.1–10 µg L^{-1}, adsorb on PAN-derived ACFs mainly through π–π stacking and hydrogen bonding at the fused ring system, with electrostatic contributions below the pKa values of the zwitterion (pH 3.3 and 7.7) [13]. Ciprofloxacin, a fluoroquinolone, shows higher q_{max} on a chitosan-modified activated carbon composite than on the unmodified carbon, attributed to complexation of the quinolone carbonyl and carboxylate groups with surface amine ligands [75]. For NSAIDs such as ibuprofen and diclofenac, the optimum lies around pH 5–6, where the undissociated form predominates and hydrophobic partitioning into ACF micropores is most effective [65].

4.4 Microplastics

Regulatory pressure on microplastics in surface water and drinking water is increasing, and domestic laundering of synthetic textiles is now recognised as a major diffuse source. An estimated 0.2–0.5 g of microfibres per kilogram of fabric is released per wash cycle, reaching municipal wastewater systems in large quantities [76], with textile-industry effluent treatment plants specifically identified as a disproportionate contributor relative to municipal systems [77]. Particle removal by carbonised nonwoven filters operates differently depending on size: larger particles are retained by size exclusion and depth filtration at inter-fibre pores, while smaller particles (below about 10 µm) are captured mainly through mechanical

straining within the internal pore network and hydrophobic interaction between the non-polar polymer surface and the carbon matrix. Because oxidised ACF surfaces and PE/PP/PS microplastics both carry a net negative charge under near-neutral conditions – the same charge mismatch that limits anionic-dye uptake in Section 4.2 – direct electrostatic attraction is unlikely to be the dominant mechanism at unmodified surfaces. Positively charged PEI- or chitosan-modified ACF surfaces, by contrast, can capture microplastics electrostatically, analogous to their effect on anionic dyes [78].

Activated-carbon-based nonwoven filters in column/fixed-bed configurations have been reported to remove more than 95% of micron-scale polystyrene microplastics [66]. Multi-stage carbon-based filtration trains, combining coarse and fine media, have been reported to improve overall microplastic capture beyond what a single stage achieves [67]. The particle load is split between stages, which also slows the pressure-drop increase that signals the need for regeneration. The published evidence base for microplastic removal by carbonised fibre filters is, however, narrow. Most studies have used model suspensions of monodisperse polystyrene or polyethylene microspheres in clean water matrices, which do not reflect the heterogeneous size distribution, irregular morphology, and complex surface chemistry of microplastics encountered in real textile effluents. The effect of co-occurring dissolved organics and surfactants on electrostatic capture efficiency has received little attention, and long-term fouling behaviour under continuous operation has not been systematically characterised. Because the values compiled below come from studies using different feed concentrations, contact times, adsorbent doses, and temperatures, Table 4 should be read as an indicative comparison of orders of magnitude rather than as a rigorous ranking of materials. Representative removal efficiencies for microplastics and other priority pollutants discussed in Sections 4.1–4.4 are summarised in Table 4.

5. Cascade Filtration and Hybrid Treatment Systems

Textile wastewater seldom contains just one type of contaminant. Heavy metals, reactive dyes, aromatic amines, suspended solids, and biological load often occur together, which makes single-stage treatment inadequate for regulatory compliance or process-water reuse. Each stage in a cascade handles a different contaminant class, and its chemistry and pore structure can be chosen accordingly. When carbonised nonwoven stages are combined with oxidative pre-treatment and downstream membrane polishing, the treatment train can in principle close the production water loop. The configurations discussed below are proposed conceptual designs, assembled from component performance reported in separate studies, rather than technologies tested as integrated systems. Table 5 summarises representative configurations discussed in the literature.

5.1 Cascade Filtration Design Principles

Good cascade design starts with feed characterisation: flow rate, suspended-solids load, chemical oxygen demand (COD) fractionation, and pollutant speciation together determine the number of stages, their order, and the surface chemistry at each layer. Working from coarse to fine is the natural sequence. An initial stage with inter-fibre pore size 100–500 µm removes macro-particles, textile fibres, and microplastics by depth filtration and inertial impaction, protecting downstream stages from rapid clogging [67]. A second stage uses oxidised or chitosan-modified ACF nonwoven with inter-fibre void dimensions of 5–50 µm to ensure adequate contact time; the actual removal of heavy metals and cationic dyes occurs by adsorption within the internal carbon micro- and

Material/precursor	*Target pollutant*	*q_{max} (mg g^{-1})*	*Removal (%)*	*pHopt*	*Ref.*
PAN-ACF nonwoven, chitosan-coated	Cu^{2+}	80–200	—	5.5	[32]
PAN-ACF nonwoven, PEI grafted	Pb^{2+}	150–280	—	5.0	[62]
Chitosan-derived N-doped carbon	Cd^{2+}	60–180	—	6.0	[63]
Viscose-ACF, HNO_3 oxidised	Hg^{2+}	50–150	—	4.5	[64]
PAN-ACF, KOH activated	Methylene blue	200–500	—	7.0	[15]
Lignin-derived ACF, CO_2 activated	Acid Orange 7	100–250	—	3.5	[27]
PAN-ACF, H_2O_2 oxidised	Tetracycline	80–200	—	5.0	[13]
Cellulose-fibre-ACF, KOH activated	Ibuprofen	70–150	—	7.0	[65]
Carbonised PAN nonwoven, O_3 oxidised	Microplastics < 100 µm	—	85–98	7.0	[66]
Cascade ACF nonwoven, three-stage	PE/PP fibres < 500 µm	—	80–95	6.5–8.5	[67]

Values are indicative ranges drawn from multiple sources and depend on initial concentration, contact time, adsorbent dose, and temperature. ACF – activated carbon fibre; PAN – polyacrylonitrile fibre; PEI – polyethylenimine; q_{max} – Langmuir maximum adsorption capacity (batch isotherm, 25°C) [13,15,27,32,62–67].

Table 4. Representative adsorption performance of carbonised textile fibre-based materials for priority pollutants in industrial wastewater treatment.

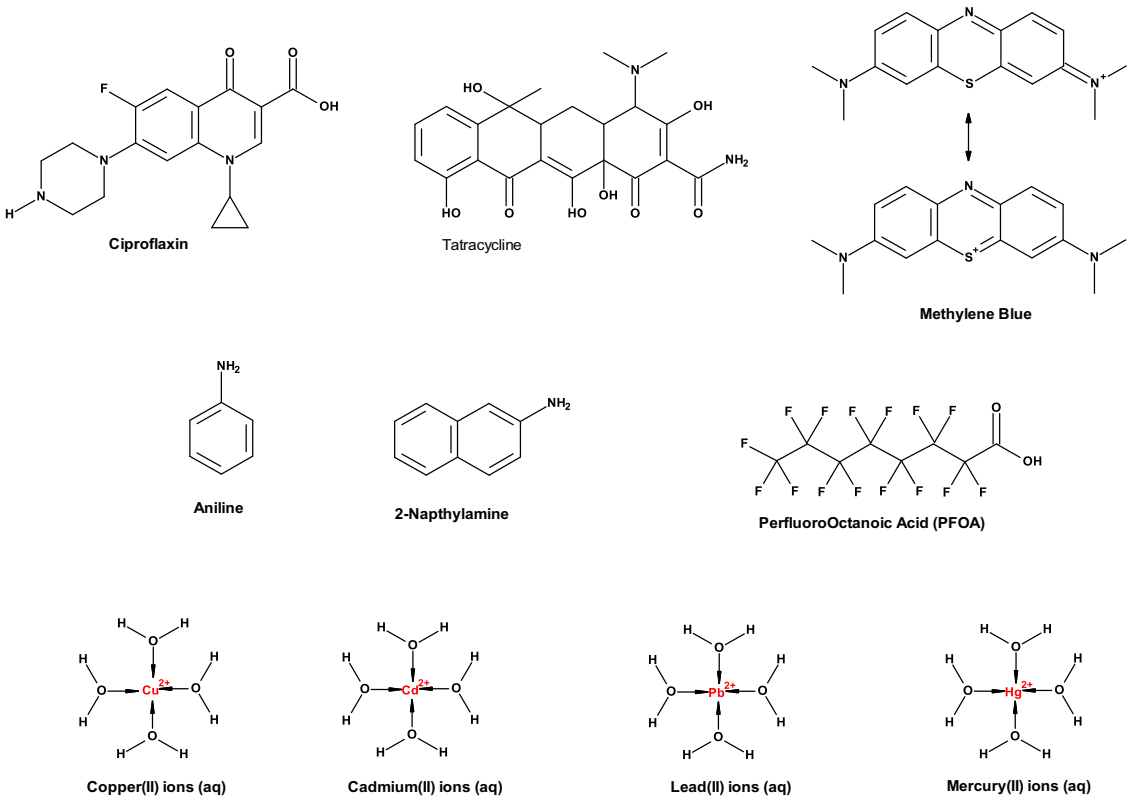


Figure 3. Representative contaminants relevant to textile wastewater treatment, including heavy metal ions, dyes, aromatic amines, pharmaceuticals, and persistent organic contaminants [7,13,15,62,68,69].

mesoporosity of the fibres, not by mechanical interception at the structural pore level. A polishing stage of N-doped ACF with BET area above 1500 m^2 g^{-1} targets trace micropollutants, aromatic amines, and pharmaceuticals [10]. As a proposed design approach rather than a validated protocol, stage mass could be sized from isotherm data at the design outlet concentration with a safety factor of 1.5–2.0 on breakthrough capacity to account for competitive adsorption in real multicomponent streams; this factor is an engineering estimate and has not itself been reported in the cited studies. It should be noted that Langmuir q_{max} values derived from batch isotherms at 25°C are not directly transferable to continuous-flow module performance; dynamic breakthrough capacity, empty-bed contact time, superficial velocity,

System configuration	***Target pollutants***	***Removal (%)***	***Other reported metrics***	***Ref.***
Two-stage cascade ACF nonwoven	Microplastics + MB dye	> 98% MP; 94% MB	—	[67]
Ozonation → ACF nonwoven	Aromatic amines, micropollutants	—	Not quantified (qualitative, see ref.)	[10]
UV/H_2O_2 → chitosan-ACF	Reactive dyes + Cu^{2+}	98% colour; 96% Cu^{2+}	—	[79]
MBR → NF membrane	COD, N, pharmaceuticals	—	Not quantified (qualitative, see ref.)	[80]
ACF cascade → RO	Complex textile effluent (mixed)	—	BOD < 10 mg L^{-1}; conductivity < 500 µS cm^{-1}	[15]
Coagulation → ACF → UF	Heavy metals + suspended solids	99% Pb^{2+}	Turbidity < 1 NTU	[81]
SBR bioreactor → ACF polishing	Residual COD + trace organics	88% micropollutants	BOD < 5 mg L^{-1}	[82]

*MBR – membrane bioreactor; SBR – sequential batch reactor; NF – nanofiltration; RO – reverse osmosis; UF – ultrafiltration; ACF – activated carbon fibre; AOP – advanced oxidation process.

Table 5. Representative cascade and hybrid treatment configurations incorporating carbonised textile fibre stages and their reported treatment performance.

and regeneration loss per cycle are the operationally relevant parameters and differ substantially from batch-derived figures. Figure 4 illustrates a conceptual treatment train, proposed here rather than reported as a tested integrated system, combining the three ACF stages with upstream oxidation and downstream membrane polishing; the individual component performance values shown are drawn from separate literature reports [10,15,67,79–82], but the train as a whole has not been validated experimentally.

Nonwoven architecture gives design freedom that granular carbon beds do not. Fibre diameter (5–20 µm), basis weight (100–500 g m^{-2}), and sheet stacking density can each be specified independently, so pressure drop, residence time, and contact area need not move together as they do in packed beds. Multi-layer stacks with graded pore structure – coarser at the inlet, finer downstream – can be formed into compact cylindrical or flat-sheet modules that fit standard industrial pressure vessels [15]. Hydraulic resistance increases approximately linearly with basis weight and decreases with mean fibre diameter, which are straightforward parameters for scale-up calculations.

5.2 Integration with Advanced Oxidation Processes

Ozonation, UV/H_2O_2, Fenton chemistry, and photocatalysis all produce hydroxyl radicals (·OH, E° = 2.80 V) capable of mineralising persistent organics that resist biological treatment and adsorption [10]. This pairing works in both directions: AOP pre-treatment converts large, non-polar dye molecules into smaller, more polar fragments that adsorb more readily on ACF, while the ACF stage concentrates residual organics and prolongs their contact with the oxidative environment [79]. ACF pre-adsorption of hydrophobic micropollutants followed by in-situ photocatalytic regeneration with TiO_2-ACF under UV can regenerate capacity without added reagents [53,54,84]. For textile effluents, ozonation at 5–15 mg L^{-1} with 5–10 min contact time typically gives more than 90% decolourisation and 40–60% COD reduction, cutting the adsorptive load on the downstream ACF stage and extending service life by a factor of 3–5 compared with direct filtration of raw effluent [10].

Fenton and photo-Fenton chemistry (Fe^{2+}/H_2O_2, pH 3–4) can mineralise persistent azo-dye degradation products more completely than ozone, but require precise pH control and produce iron sludge as a secondary waste. Fe_3O_4-functionalised ACF nonwovens used as heterogeneous Fenton catalysts shift the working pH to

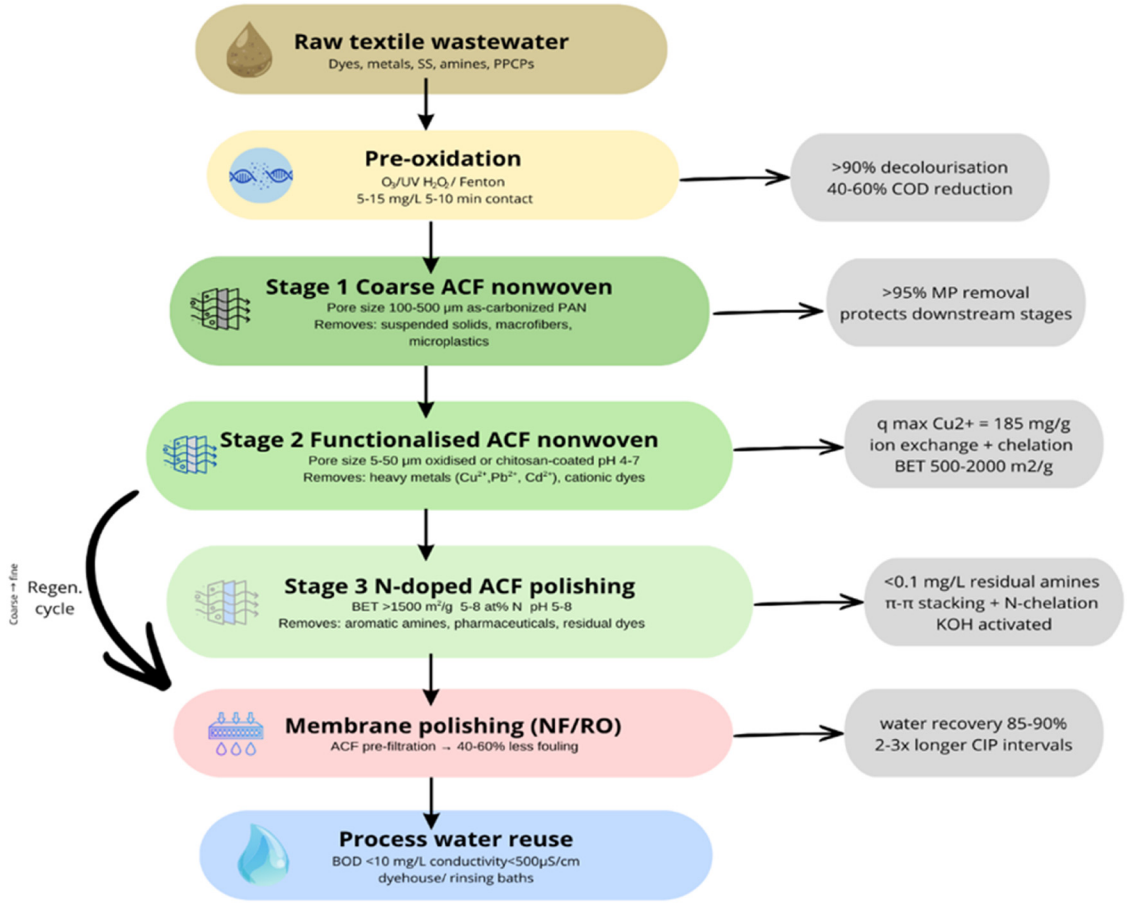


Figure 4. Schematic of a multi-stage cascade treatment train for textile wastewater incorporating pre-oxidation, three ACF nonwoven filter stages, and membrane polishing [10,15,79–83].

5.5–6.5, removing the need for acidification and neutralisation steps and cutting sludge production [55]. Residual H_2O_2 must be quenched or decomposed before the water reaches downstream RO membranes since oxidant carry-over causes irreversible membrane damage.

5.3 Integration with Membrane and Biological Processes

Where the goal is effluent of sufficient quality for reuse in dyeing or rinsing, membrane polishing – MF, UF, NF, or RO depending on the required separation – is the logical final step. Their main operational vulnerability is fouling: colloidal organics, surfactants, scaling salts, and biofilms raise transmembrane pressure, reduce permeate flux, and shorten service life [80,85]. ACF pre-filtration removes the colloidal fraction by size exclusion (in pores below 0.1 μm), reduces dissolved organic carbon by adsorption, and strips out the most surface-active species that initiate gel-layer fouling, allowing NF and RO to run at lower pressure and with longer intervals between cleaning events [15]. Studies on pre-treatment of secondary effluents before membrane filtration have reported substantially lower normalised flux decline rates and extended CIP intervals compared with direct membrane operation [81], though the magnitude of benefit varies with feed composition and the specific ACF configuration used.

In a membrane bioreactor (MBR), activated sludge or biofilm treatment is combined with in-line MF or UF in a single vessel. The secondary clarifier is eliminated, and the permeate is already clarified to a standard suitable for NF or RO polishing. Placing carbonised ACF nonwoven stages inside the MBR aeration tank – as structured carriers that double as biofilm support and adsorbent – has been reported to buffer peak organic loading on the membrane module and to protect the biomass from inhibitory compounds such as heavy metals and biocidal dyes that would otherwise suppress biological activity [82]. Fill-draw SBR operation suits ACF filter integration well. During the quiescent decant phase, suspended biomass settles and the ACF stage can be run under gravity-driven flow with little risk of biomass fouling.

6. Challenges, Circular Economy Perspectives, and Conclusions

6.1 Regeneration and Fouling

ACF nonwovens cost roughly three to five times more per unit mass than granular activated carbon [11], which makes regeneration an economic necessity rather than an optional step. Three main routes exist.

Thermal treatment at 700–900°C in steam or CO_2 pyrolyses the adsorbed organic layer and restores more than 90% of initial capacity, but each cycle burns off 5–10% of the carbon mass at pore edges, so cumulative micropore loss is significant over time [36]. It is important to distinguish these two figures: the >90% recovery refers to the specific (mass normalised) adsorption capacity of the carbon that remains after regeneration, not to the total capacity of the filter element. Because 5–10% of the carbon mass is lost at each thermal cycle, the total capacity of the element declines cumulatively – roughly by a factor of $(0.90–0.95)^n$ after n cycles – even though the per-gram performance of the surviving material is largely preserved, a distinction long recognised for granular activated carbon, where progressively more make-up carbon must be added over successive cycles even as per-unit-weight capacity recovery remains high [86]. Service-life projections in Sections 6.2 and 6.4 should therefore be based on cumulative mass loss of the element, not on the per-cycle capacity-recovery figure alone.

Acid-alkali washing – sequential rinse with HCl or H_2SO_4 at pH 2 to strip metal ions by proton competition, followed by NaOH at pH 12 to restore surface charge – suits metal-laden stages and avoids high-temperature structural damage, though it produces concentrated eluates requiring further treatment [29]. In-situ photocatalytic regeneration of TiO_2-bearing ACF nonwovens under UV irradiation sidesteps both thermal cycling and chemical reagent use, but works only for compounds that ·OH can oxidise and requires optically transparent housings that trade off against mechanical robustness [53,54].

A critical gap in the published record concerns long-term stability under industrially representative conditions. To the authors' knowledge, identified regeneration studies rarely extend beyond 20–30 cycles, and none have sustained real textile effluent as feed throughout; stable adsorption performance of functionalised ACF nonwovens across more than 50 regeneration cycles under industrially representative conditions has not been documented in the reviewed literature. Whether surface coatings – PEI grafts, crosslinked chitosan layers, sol-gel nanoparticle deposits – retain structural and chemical integrity through the repeated pH swings (pH 2–12) and elevated temperatures (up to 60°C) of industrial acid–alkali cleaning sequences remains unanswered. This is not a minor technical detail: without credible service-life data covering at least 50 cycles, an operator cannot project consumable costs or size a replacement inventory, which in practice means the technology cannot clear a basic economic feasibility review.

Fouling – contaminant accumulation that backwashing does not fully reverse – is the other main cause of performance decline in continuous-flow operation. In practice, it does not happen all at once. Surface-active organics and humic-like substances are taken up rapidly at primary adsorption sites within the first few hours of operation. Over the following days, colloidal particles and macromolecules work their way into mesopores. Microbial colonisation develops on the timescale of weeks, gradually blocking surface area and reducing permeability [87]. Nano-Ag or nano-Cu functionalisation limits the biological stage, but the earlier two phases call for hydraulic or chemical intervention. Backwash protocols that combine upward-flow water jets with air-scour restore 80–95% of initial permeability if applied at the first measurable rise in pressure, but their effect diminishes

once a compressible colloidal cake has formed [88].

6.2 Scale-Up Challenges

Batch laboratory data systematically overpredict performance in pilot-scale continuous-flow systems, and the discrepancy is not always discussed honestly in the literature. Axial dispersion and channelling in multi-layer nonwoven stacks reduce effective contact time below the design value. Non-uniform flow distribution in large-area modules (above 1 m^2) arises from pressure gradients in feed manifolds. Elevated operating temperatures (40–60°C, typical of textile process streams) shift adsorption equilibria and can degrade polymer coatings [5]. Pilot trials on real textile effluents consistently report capacities 30–50% below laboratory isotherm predictions, attributed to competitive adsorption from background dissolved organic matter and to kinetic limitations at industrial flow velocities [43]. The membrane sector has workable pilot-testing and techno-economic frameworks; similar tools for ACF cascade systems do not yet exist, and their absence is a practical obstacle to industrial adoption.

6.3 Circular Economy Perspectives

These materials fit within circular-economy logic on two separate counts. Using sorted cotton-polyester waste, PAN-based acrylic scrap, or crustacean-processing residues as carbonisation feedstocks converts end-of-life waste into functional filter media, avoiding both landfilling and the energy-intensive production of virgin activated carbon from coal or coconut shell [28]. LCA comparisons generally show lower global warming potential and cumulative energy demand for waste-derived carbons than for coal-based GAC [89], though the margin narrows when feedstock sorting and pre-treatment are energy-intensive. The environmental benefit case, however, rests on the assumption of controlled feedstock composition. Post-consumer textile waste arrives as polydisperse blends of unknown fibre-type ratios, variable dyestuff loads, and residual finishing chemicals; each of these parameters shifts the optimal carbonisation temperature and the surface chemistry of the product. Without upstream sorting to textile-grade homogeneity – a step that is costly and not yet widely available at collection scale – the environmental and performance claims made for waste-derived ACF feedstocks should be treated with caution. On the water side, treating process effluent to reuse quality closes or partially closes the production water loop. A plant treating 300 m^3 day^{-1} with 80% water recovery, for instance, would avoid abstracting roughly 240 m^3 day^{-1} of freshwater and discharging the equivalent volume as polluted effluent – a benefit that grows as water tariffs and discharge fees rise.

A dedicated economic assessment of this pathway is largely absent from the literature and remains an important gap. Techno-economic feasibility of textile-waste-derived activated carbon is explicitly flagged as an open research need [90], and cost data specific to carbon fibre production from textile-waste feedstocks are only beginning to emerge: a recent techno-economic analysis of carbon fibre made from recycled acrylic textile waste reported approximately 20% lower production cost than virgin-precursor carbon fibre at 50% recycled content, alongside a roughly 40% reduction in cradle-to-gate greenhouse-gas emissions [91]. These figures concern fibre production rather than the full cascade filtration system discussed here, and do not include downstream costs such as activation, module fabrication, regeneration, or comparison against conventional treatment trains (coagulation, granular activated carbon, membrane processes). A dedicated techno-economic and comparative cost analysis of carbonised-fibre cascade filtration against these established alternatives is therefore identified as a priority for future work before the concept proposed here could be assessed for practical industrial adoption.

The spent adsorbent from chemical regeneration cycles carries concentrated heavy metals, dye fragments, and degradation products that themselves require management. Thermal regeneration recovers the carbon for reuse and concentrates inorganics in the ash residue, which may be worth processing by hydrometallurgical routes for copper, lead, or zinc recovery if concentrations are high enough [92]. Alkali eluates from chitosan-coated stages tend to be ammonium-rich; these can in principle be treated by nitrification-denitrification before discharge, integrating the regeneration circuit into the plant's broader wastewater management.

6.4 Conclusions and Future Perspectives

The picture that emerges from this review is uneven: the materials science is well-developed, but the path to industrial deployment remains obstructed by gaps in long-term performance data and the absence of standardised evaluation tools.

- For continuous-flow ACF nonwovens, PAN continues to give the most predictable combination of surface area, microporosity, and mechanical strength [14,16,24]. Cellulose fibres, chitosan fibres, and lignocellulosic materials carry useful surface chemistries for specific contaminant classes and have real cost and environmental advantages, but carbon yield and structural reproducibility from these precursors remain below what PAN delivers [27,30,68].
- As-carbonised fibres without modification cover a narrow contaminant range. Oxidative treatment, polymer grafting, nanoparticle deposition, and nitrogen doping each extend performance into different areas of the pollutant spectrum [44,51,58]. Whether complex composite coatings hold up through many regeneration cycles is a practical question that the literature has not yet answered convincingly [29,36]. Identified cycle tests typically stop at 10–20 iterations using synthetic single-contaminant feeds, which is an insufficient basis for projecting operational service life in an industrial setting.
- Multi-stage ACF cascades can reach the effluent quality needed for

process-water reuse, but only when combined with upstream oxidation and downstream membrane polishing [10,15,80]. No single stage achieves this on its own and claims to that effect in the literature should be read critically.

- Industrial uptake remains slow. ACF nonwovens cost 3–5 times more than granular carbon [11], real-effluent performance falls 30–50% short of laboratory isotherm projections [5,43], and there are no standardised testing or techno-economic tools that would let an end-user build a credible business case. Until those tools exist, the technology is unlikely to move beyond pilot demonstrations at scale.
- Rising virgin raw-material costs and increasing discharge charges are gradually improving the economics of waste-derived filter media and closed production water loops, without requiring any change in the regulatory framework [28,89].

Three gaps stand out as priorities for future work: continuous carbonisation and activation processes suitable for variable-composition waste-textile feedstocks at production scale [34]; systematic characterisation of competitive adsorption and fouling kinetics under realistic, dynamic multicomponent flow conditions, since most published data still rely on idealised single-contaminant batches [5,43]; and accelerated ageing protocols capable of supporting credible service-life predictions and regulatory acceptance [29,36].

7. Abbreviations

The following abbreviations are used in this manuscript:

ACF	Activated Carbon Fibre
ACFs	Activated Carbon Fibres
CAN	Activated Carbon Nonwoven
ACNs	Activated Carbon Nonwovens
AOP	Advanced Oxidation Process
AOPs	Advanced Oxidation Processes
BET	Brunauer-Emmett-Teller (specific surface area method)
BOD	Biochemical Oxygen Demand
CED	Cumulative Energy Demand
CIP	Cleaning-In-Place
CNF	Cellulose Nanofibre
CNC	Cellulose Nanocrystal
COD	Chemical Oxygen Demand
DD	Degree of Deacetylation
DOC	Dissolved Organic Carbon
EU	European Union
GAC	Granular Activated Carbon
GWP	Global Warming Potential
LCA	Life Cycle Assessment
MB	Methylene Blue
MBR	Membrane Bioreactor
MF	Microfiltration
MP	Microplastics
NF	Nanofiltration
NSAIDs	Non-Steroidal Anti-Inflammatory Drugs
N-PC	Nitrogen-Doped Porous Carbon
N-PCs	Nitrogen-Doped Porous Carbons
PAN	Polyacrylonitrile Fibre
PPCPs	Pharmaceuticals and Personal Care Products
PE	Polyethylene
PEI	Polyethylenimine
PS	Polystyrene
q_{max}	Maximum Adsorption Capacity (Langmuir Isotherm)
REACH	Registration, Evaluation, Authorisation and Restriction of Chemicals
RO	Reverse Osmosis
ROS	Reactive Oxygen Species
SBR	Sequential Batch Reactor
SMEs	Small and Medium-Sized Enterprises
TiO_2	Titanium Dioxide
UF	Ultrafiltration
UV	Ultraviolet Radiation
VOCs	Volatile Organic Compounds
Fe_3O_4	Magnetite (Iron Oxide)

Acknowledgements

This work was completed while one of the authors (M.G) was a doctoral student at the Interdisciplinary Doctoral School of the Lodz University of Technology in Poland.

Funding information

This work was supported by the Ministry of Science and Higher Education, Poland, under project Science for Society II "Water, a priceless resource – actions for its protection, number, NdS-II/SN/0269/2023/01.

Author contributions

Conceptualisation, M.H.K.; literature survey and data curation, M.H.K., Z.M., M.G., M.S.; writing-original draft preparation, M.H.K., Z.M., M.G., and M.S.; writing-review and editing, M.H.K., Z.M., M.G., M.S., I.K.-K., J.O., A.W., and R.Ż. All authors have read and agreed to the published version of the manuscript.

Conflict of interest statement

The authors declare no conflicts of interest.

Ethical approval

Not applicable.

Consent to participate

All authors have read the submitted version.

Consent to publish

All authors have and approved the submitted version for publication.

Data availability statement

Not applicable.

References

[1] Partnerships and cooperation for water | UN World Water Development Report 2023 n.d. https://www.unesco.org/reports/wwdr/2023/en (accessed May 25, 2026).

[2] GUS. Statistical analyses 2022.

[3] Hasanbeigi A., Price L. A technical review of emerging technologies for energy and water efficiency and pollution reduction in the textile industry. J. Clean. Prod., 2015; 95: 30–44. doi: 10.1016/J.JCLEPRO.2015.02.079.

[4] Oatley-Radcliffe D. L., Walters M., Ainscough T. J., Williams P. M., Mohammad A. W., Hilal N. Nanofiltration membranes and processes: A review of research trends over the past decade. J. Water Process. Eng., 2017; 19: 164–71. doi: 10.1016/J.JWPE.2017.07.026.

[5] Holkar C. R., Jadhav A. J., Pinjari D. V., Mahamuni N. M., Pandit A. B. A critical review on textile wastewater treatments: Possible approaches. J. Env. Manage, 2016; 182: 351–66. doi: 10.1016/J.JENVMAN.2016.07.090.

[6] Lellis B., Fávaro-Polonio C. Z., Pamphile J. A., Polonio J. C. Effects of textile dyes on health and the environment and bioremediation potential of living organisms. Biotechnol. Res., 2019; 3: 275–90. doi: 10.1016/J.BIORI.2019.09.001.

[7] Brüschweiler B. J., Merlot C. Azo dyes in clothing textiles can be cleaved into a series of mutagenic aromatic amines which are not regulated yet. Regul. Toxicol. Pharmacol., 2017; 88: 214–26.

[8] De Aragão Umbuzeiro G., Freeman H. S., Warren S. H., De Oliveira D. P., Terao Y., Watanabe T., et al. The contribution of azo dyes to the mutagenic activity of the Cristais River. Chemosphere, 2005; 60: 55–64. doi: 10.1016/J.CHEMOSPHERE.2004.11.100.

[9] Edebali Ö, Krupčíková S., Goellner A., Vrana B., Muz M., Melymuk L. Tracking aromatic amines from sources to surface waters. Env. Sci. Technol. Lett., 2024; 11: 397–409. doi: 10.1021/acs.estlett.4c00032.

[10] Paździor K., Bilińska L., Ledakowicz S. A review of the existing and emerging technologies in the combination of AOPs and biological processes in industrial textile wastewater treatment. Chem. Eng. J., 2019; 376. doi: 10.1016/J.CEJ.2018.12.057.

[11] Crini G., Lichtfouse E. Advantages and disadvantages of techniques used for wastewater treatment. Env. Chem. Lett., 2018; 17: 145–55. doi: 10.1007/S10311-018-0785-9.

[12] Bhatnagar A., Sillanpää M. Utilization of agro-industrial and municipal waste materials as potential adsorbents for water treatment-A review. Chem. Eng. J., 2010; 157: 277–96. doi: 10.1016/J.CEJ.2010.01.007.

[13] Ahmed M. B., Zhou J. L., Ngo H. H., Guo W. Adsorptive removal of antibiotics from water and wastewater: Progress and challenges. Sci. Total. Env., 2015; 532: 112–26. doi: 10.1016/j.scitotenv.2015.05.130.

[14] Ko T. H., chiranairadul P., Lu C. K., Lin C. H. The effects of activation by carbon dioxide on the mechanical properties and structure of PAN-based activated carbon fibers. Carbon N. Y., 1992; 30: 647–55. doi: 10.1016/0008-6223(92)90184-X.

[15] Brasquet C., Le Cloirec P. Adsorption onto activated carbon fibers: Application to water and air treatments. Carbon N. Y., 1997; 35: 1307–13. doi: 10.1016/S0008-6223(97)00079-1.

[16] Frank E., Hermanutz F., Buchmeiser M. R. Carbon fibers: Precursors, manufacturing, and properties. Macromol. Mater. Eng., 2012; 297: 493–501. doi: 10.1002/MAME.201100406.

[17] Bajaj P., Roopanwal A. K. Thermal stabilization of acrylic precursors for the production of carbon fibers: an overview. J. Macromol. Sci. Part. C. Polym. Rev., 1997; 37: 97–147. doi: 10.1080/15321799708014734.

[18] Zhu C., Liu P., Mathew A. P. Self-Assembled TEMPO Cellulose Nanofibers: Graphene Oxide-Based Biohybrids for Water Purification. ACS Appl. Mater. Interfaces, 2017; 9: 21048–58. doi: 10.1021/ACSAMI.7B06358.

[19] Foong S. Y., Liew R. K., Yek P. N. Y., Chan Y. H., Lam S. S. A review in production of nitrogen-enriched carbon materials via chitin pyrolysis and activation for enhanced wastewater remediation. Curr. Opin. Green. Sustain. Chem., 2024; 47: 100920. doi: 10.1016/j.cogsc.2024.100920.

[20] Kim C. W., Kim D. S., Kang S. Y., Marquez M., Joo Y. L. Sorption properties of the composite fibers made of PAN and chitosan. J. Appl. Polym. Sci., 2002; 84: 2505–11. doi: 10.1002/app.10660.

[21] Mirza N. R., Huang R., Du E., Peng M., Pan Z., Ding H., Shan G., Ling L., Xie Z. A review of the textile wastewater treatment technologies with special focus on advanced oxidation processes (AOPs), membrane separation and integrated AOP-membrane processes. Desalin Water Treat., 2020; 206: 83–107.

[22] Afonso C., Silveira J. E., Zazo J. A., Fernandes A. Sustainable water reuse in textile processing: a hybrid nanofiltration-reverse osmosis-persulfate oxidation treatment approach. Text. Res. J., 2026. doi: 10.1177/00405175261449433.

[23] Pundir A., Thakur M. S., Radha, Goel B., Prakash S., Kumari N., et al. Innovations in textile wastewater management: a review of zero liquid discharge technology. Env. Sci. Pollut. Res., 2024; 31: 12597–616. doi: 10.1007/s11356-024-31827-y.

[24] Rahaman M. S. A., Ismail A. F., Mustafa A. A review of heat treatment on polyacrylonitrile fiber. Polym. Degrad. Stab., 2007; 92: 1421–32. doi: 10.1016/J.POLYMDEGRADSTAB.2007.03.023.

[25] Ouyang Q., Cheng L., Wang H., Li K. Mechanism and kinetics of the stabilization reactions of itaconic acid-modified polyacrylonitrile. Polym. Degrad. Stab., 2008; 93: 1415–21. doi: 10.1016/J.POLYMDEGRADSTAB.2008.05.021.

[26] Yin J., Zhang W., Alhebshi N. A., Salah N., Alshareef H. N. Synthesis Strategies of Porous Carbon for Supercapacitor Applications. Small Methods, 2020; 4: 1900853.

[27] Suhas, Carrott P. J. M., Ribeiro Carrott M. M. L. Lignin – from natural adsorbent to activated carbon: A review. Bioresour. Technol., 2007; 98: 2301–12. doi: 10.1016/J.BIORTECH.2006.08.008.

[28] Ragauskas A. J., Beckham G. T., Biddy M. J., Chandra R., Chen F., Davis M. F., et al. Lignin valorization: Improving lignin processing in the biorefinery. Science, 2014; 80: 344. doi: 10.1126/SCIENCE.1246843.

[29] Suzuki M. Activated carbon fiber: Fundamentals and applications. Carbon N. Y., 1994; 32: 577–86. doi: 10.1016/0008-6223(94)90075-2.

[30] Byrne C. E., Nagle D. C. Carbonization of wood for advanced materials applications. Carbon N. Y., 1997; 35: 259–66. doi: 10.1016/S0008-6223(96)00136-4.

[31] Wan C., Li J. Cellulose aerogels functionalized with polypyrrole and silver nanoparticles: In-situ synthesis, characterization and antibacterial activity. Carbohydr. Polym., 2016; 46: 362–7. doi: 10.1016/J.CARBPOL.2016.03.081.

[32] Yuan X., An N., Zhu Z., Sun H., Zheng J., Jia M., Lu C., Zhang W., Liu N. Hierarchically porous nitrogen-doped carbon materials as efficient adsorbents for removal of heavy metal ions. Process. Saf. Env. Prot., 2018; 119: 320–9. doi: 10.1016/j.psep.2018.08.012.

[33] Wan Ngah W. S., Teong L. C., Hanafiah MAKM. Adsorption of dyes and heavy metal ions by chitosan composites: A review. Carbohydr. Polym., 2011; 83: 1446–56.

[34] Phan N. H., Rio S., Faur C., Le Coq L., Le Cloirec P., Nguyen T. H. Production of fibrous activated carbons from natural cellulose (jute, coconut) fibers for water treatment applications. Carbon N. Y., 2006; 44: 2569–77. doi: 10.1016/J.CARBON.2006.05.048.

[35] Babel K., Jurewicz K. KOH activated carbon fabrics as supercapacitor material. J. Phys. Chem. Solids, 2004; 65: 275–80. doi: 10.1016/j.jpcs.2003.08.023.

[36] Marsh H., Rodríguez-Reinoso F. Activated Carbon. Act. Carbon, 2006; 1–536. doi: 10.1016/B978-0-08-044463-5.X5013-4.

[37] Inagaki M., Kang F. Materials Science and Engineering of Carbon: Fundamentals. Mater. Sci. Eng. Carbon Fundam. Second. Ed., 2014; 1–539. doi: 10.1016/C2013-0-13699-9.

[38] Kim M. A., Jang D., Tejima S., Cruz-Silva R., Joh H. I., Kim H. C., et al. Strengthened PAN-based carbon fibers obtained by slow heating rate carbonization. Sci. Rep., 2016; 6: 22988. doi: 10.1038/srep22988.

[39] Huang X. Fabrication and Properties of Carbon Fibers. Mater, 2009; 2: 2369–2403. doi: 10.3390/MA2042369.

[40] Deng J., Li M., Wang Y. Biomass-derived carbon: Synthesis and applications in energy storage and conversion. Green. Chem., 2016; 18: 4824–54. doi: 10.1039/C6GC01172A.

[41] Bacon R. Carbon Fibers from Rayon Precursors. In: Walker P. L. J., Thrower P. A., editors. Chem. Phys. Carbon, vol. 9, New York: Marcel Dekker; 1973, p. 1–102.

[42] Bengisu M., Yilmaz E. Oxidation and pyrolysis of chitosan as a route for carbon fiber derivation. Carbohydr. Polym., 2002; 50: 165–75. doi: 10.1016/S0144-8617(02)00018-8.

[43] Moreno-Castilla C. Adsorption of organic molecules from aqueous solutions on carbon materials. Carbon N. Y., 2004; 42: 83–94. doi: 10.1016/J.CARBON.2003.09.022.

[44] Figueiredo J. L., Pereira M. F. R., Freitas M. M. A., Órfão J. J. M. Modification of the surface chemistry of activated carbons. Carbon N. Y., 1999; 37: 1379–89. doi: 10.1016/S0008-6223(98)00333-9.

[45] Wang Y., Shi L., Gao L., Wei Q., Cui L., Hu L., et al. The removal of lead ions from aqueous solution by using magnetic hydroxypropyl chitosan/oxidized multiwalled carbon nanotubes composites. J. Colloid Interface Sci., 2015; 451: 7–14. doi: 10.1016/J.JCIS.2015.03.048.

[46] Rouquerol J., Llewellyn P., Rouquerol F. Is the bet equation applicable to microporous adsorbents? Stud. Surf. Sci. Catal., 2007; 160: 49–56. doi: 10.1016/S0167-2991(07)80008-5.

[47] Fitzer E. Pan-based carbon fibers-present state and trend of the technology from the viewpoint of possibilities and limits to influence and to control the fiber properties by the process parameters. Carbon N. Y., 1989; 27: 621–45. doi: 10.1016/0008-6223(89)90197-8.

[48] Ferrari A., Robertson J. Interpretation of Raman spectra of disordered and amorphous carbon. Phys. Rev. B, 2000; 61: 14095. doi: 10.1103/PhysRevB.61.14095.

[49] Donnet J.-B., Chand Bansal R. Carbon Fibers 1998. doi: 10.1201/9781482285390.

[50] Shim J. W., Park S. J., Ryu S. K. Effect of modification with HNO3 and NaOH on metal adsorption by pitch-based activated carbon fibers. Carbon, 2001; 39: 1635–42. doi: 10.1016/S0008-6223(00)00290-6.

[51] Pan B., Pan B., Zhang W., Lv L., Zhang Q., Zheng S. Development of polymeric and polymer-based hybrid adsorbents for pollutants removal from waters. Chem. Eng. J., 2009; 151: 19–29. doi: 10.1016/J.CEJ.2009.02.036.

[52] Huang C. C., Su Y. J. Removal of copper ions from wastewater by adsorption/electrosorption on modified activated carbon cloths. J. Hazard. Mater., 2010; 175: 477–83. doi: 10.1016/j.jhazmat.2009.10.030.

[53] Fu P., Luan Y., Dai X. Preparation of activated carbon fibers supported TiO2 photocatalyst and evaluation of its photocatalytic reactivity. J. Mol. Catal. A Chem. 2004; 221: 81–8. doi: 10.1016/J.MOLCATA.2004.06.018.

[54] Fujishima A., Zhang X., Tryk D. A. TiO_2 photocatalysis and related surface phenomena. Surf. Sci. Rep. 2008; 63: 515–82. doi: 10.1016/J.SURFREP.2008.10.001.

[55] Xu P., Zeng G. M., Huang D. L., Feng C. L., Hu S., Zhao M. H., et al. Use of iron oxide nanomaterials in wastewater treatment: A review. Sci. Total. Env., 2012; 424: 1–10. doi: 10.1016/j.scitotenv.2012.02.023.

[56] Rai M., Yadav A., Gade A. Silver nanoparticles as a new generation of antimicrobials. Biotechnol. Adv., 2009; 27: 76–83. doi: 10.1016/j.biotechadv.2008.09.002.

[57] Kalantzi I., Mylona K., Toncelli C., Bucheli T. D., Knauer K., Pergantis S.

A., Pitta P., Tsiola A., Tsapakis M. Ecotoxicity of silver nanoparticles on plankton organisms: a review. J. Nanopart. Res., 2019; 21: 65. doi: 10.1007/s11051-019-4504-7.

[58] Liang H. W., Zhuang X., Brüller S., Feng X., Müllen K. Hierarchically porous carbons with optimized nitrogen doping as highly active electrocatalysts for oxygen reduction. Nat. Commun., 2014; 5: 4973.

[59] Matter P. H., Zhang L., Ozkan U. S. The role of nanostructure in nitrogen-containing carbon catalysts for the oxygen reduction reaction. J. Catal., 2006; 239: 83–96. doi: 10.1016/J.JCAT.2006.01.022.

[60] Xia Y., Mokaya R., Walker G. S., Zhu Y. Superior CO_2 adsorption capacity on N-doped, high-surface-area, microporous carbons templated from zeolite. Adv. Energy Mater., 2011; 1: 678–83. doi: 10.1002/AENM.201100061;REQUESTEDJOURNAL:JOURNAL:16146840;WGROUP:STRING:PUBLICATION.

[61] Bhatnagar A., Hogland W., Marques M., Sillanpää M. An overview of the modification methods of activated carbon for its water treatment applications. Chem. Eng. J., 2013; 219: 499–511. doi: 10.1016/J.CEJ.2012.12.038.

[62] Varma A. J., Deshpande S. V., Kennedy J. F. Metal complexation by chitosan and its derivatives: a review. Carbohydr. Polym., 2004; 55: 77–93. doi: 10.1016/J.CARBPOL.2003.08.005.

[63] Boamah P. O., Huang Y., Hua M., Zhang Q., Wu J., Onumah J., et al. Sorption of heavy metal ions onto carboxylate chitosan derivatives-A mini-review. Ecotoxicol. Env. Saf., 2015; 116: 113–20. doi: 10.1016/j.ecoenv.2015.01.012.

[64] Bandosz T. Activated Carbon Surfaces in Environmental Remediation Vol. 298. Elsevier; 2006: pp. 500–3.

[65] Guedidi H., Reinert L., Soneda Y., Bellakhal N., Duclaux L. Adsorption of ibuprofen from aqueous solution on chemically surface-modified activated carbon cloths. Arab. J. Chem., 2017; 10: S3584–94. doi: 10.1016/j.arabjc.2014.03.007.

[66] Amirah Mohd Napi N. N., Ibrahim N., Adli Hanif M., Hasan M., Dahalan F. A., Syafiuddin A., Boopathy R. Column-based removal of high concentration microplastics in synthetic wastewater using granular activated carbon. Bioengineered, 2023; 14: 2276391. doi: 10.1080/21655979.2023.2276391.

[67] Sarsour J., Ewert B., Janisch B., Stegmaier T., Gresser G. T. Efficient Filtration Systems for Microplastic Elimination in Wastewater. Microplastics, 2025; 4: 36. doi: 10.3390/microplastics4030036.

[68] Guibal E. Interactions of metal ions with chitosan-based sorbents: a review. Sep. Purif. Technol., 2004; 38: 43–74. doi: 10.1016/J.SEPPUR.2003.10.004.

[69] Peng X., Hu F., Lam F. L. Y., Wang Y., Liu Z., Dai H. Adsorption behavior and mechanisms of ciprofloxacin from aqueous solution by ordered mesoporous carbon and bamboo-based carbon. J. Colloid Interface Sci., 2015; 460: 349–60. doi: 10.1016/J.JCIS.2015.08.050.

[70] Kuo C. Y. Comparison with as-grown and microwave modified carbon nanotubes to removal aqueous bisphenol A. Desalination, 2009; 249: 976–82. doi: 10.1016/J.DESAL.2009.06.058.

[71] Zhu L., Xi M., Yao Y., Lan P. Thiol-functionalized activated carbon fibers as efficient adsorbents. Mater. Chem. Phys., 2023; 302: 127552. doi: 10.1016/j.matchemphys.2023.127552.

[72] Vakili M., Rafatullah M., Salamatinia B., Abdullah A. Z., Ibrahim M. H., Tan K. B., et al. Application of chitosan and its derivatives as adsorbents for dye removal from water and wastewater: A review. Carbohydr. Polym., 2014; 113: 115–30. doi: 10.1016/j.carbpol.2014.07.007.

[73] Guibal E., Touraud E., Roussy J. Chitosan Interactions with Metal Ions and Dyes: Dissolved-state vs. Solid-state Application. World J. Microbiol. Biotechnol. 2005 216 2005; 21: 913–20. doi: 10.1007/S11274-004-6559-5.

[74] Li K., Li Y., Zheng Z. Kinetics and mechanism studies of p-nitroaniline adsorption on activated carbon fibers prepared from cotton stalk by $NH_4H_2PO_4$ activation and subsequent gasification with steam. J. Hazard. Mater., 2010; 178: 553–9. doi: 10.1016/j.jhazmat.2010.01.120.

[75] Malakootian M., Nasiri A., Mahdizadeh H. Preparation of $CoFe_2O_4$/activated carbon@chitosan as a new magnetic nanobiocomposite for adsorption of ciprofloxacin in aqueous solutions. Water Sci. Technol., 2018; 78: 2158–70. doi: 10.2166/wst.2018.494.

[76] Pirc U., Vidmar M., Mozer A., Kržan A. Emissions of microplastic fibers from microfiber fleece during domestic washing. Env. Sci. Pollut. Res. Int., 2016; 23: 22206–11. doi: 10.1007/S11356-016-7703-0.

[77] Ramasamy R., Aragaw T. A., Balasaraswathi Subramanian R. Wastewater treatment plant effluent and microfiber pollution: focus on industry-specific wastewater. Env. Sci. Pollut. Res., 2022; 29: 51211–33. doi: 10.1007/s11356-022-20930-7.

[78] Ali A., Militky J. Activated carbon for the removal of micro-plastics from wastewater: a review. Appl. Water Sci., 2026; 16: 222. doi: 10.1007/s13201-026-02906-x.

[79] Andreozzi R., Marotta R., Paxéus N. Pharmaceuticals in STP effluents and their solar photodegradation in aquatic environment. Chemosphere, 2003; 50: 1319–30. doi: 10.1016/S0045-6535(02)00769-5.

[80] Meng F., Chae S. R., Drews A., Kraume M., Shin H. S., Yang F. Recent advances in membrane bioreactors (MBRs): Membrane fouling and membrane material. Water Res., 2009; 43: 1489–512. doi: 10.1016/J.WATRES.2008.12.044.

[81] Shon H. K., Vigneswaran S., Kim I. S., Cho J., Ngo H. H. Effect of pretreatment on the fouling of membranes: Application in biologically treated sewage effluent. J. Memb. Sci., 2004; 234: 111–20. doi: 10.1016/J.MEMSCI.2004.01.015.

[82] Huang X., Gui P., Qian Y. Effect of sludge retention time on microbial behaviour in a submerged membrane bioreactor. Process. Biochem., 2001; 36: 1001–6. doi: 10.1016/S0032-9592(01)00135-2.

[83] Talvitie J., Mikola A., Koistinen A., Setälä O. Solutions to microplastic pollution – Removal of microplastics from wastewater effluent with advanced wastewater treatment technologies. Water

Res., 2017; 123: 401–7. doi: 10.1016/j.watres.2017.07.005.

[84] Matos J., Laine J., Herrmann J. M. Synergy effect in the photocatalytic degradation of phenol on a suspended mixture of titania and activated carbon. Appl. Catal. B Env., 1998; 18: 281–91. doi: 10.1016/S0926-3373(98)00051-4.

[85] Vatanpour V., Madaeni S. S., Moradian R., Zinadini S., Astinchap B. Novel antibifouling nanofiltration polyethersulfone membrane fabricated from embedding TiO_2 coated multiwalled carbon nanotubes. Sep. Purif. Technol., 2012; 90: 69–82. doi: 10.1016/J.SEPPUR.2012.02.014.

[86] Martin R. J., Ng W. J. The thermal regeneration of exhausted activated carbon: the balance between weight loss and regeneration efficiency. In: Pawlowski L., Lacy W. J., Dlugosz J. J., editors. Chemistry for the Protection of the Environment. Environmental Science Research, vol. 42, Springer, Boston, MA; 1991. p. 427–38. doi: 10.1007/978-1-4615-3282-8_36.

[87] Crittenden J. C., Trussell R. R., Hand D. W., Howe K. J., Tchobanoglous G., Borchardt J. H. MWH's Water Treatment: Principles and Design, 3rd Edn. 2012; pp. 1–1901. doi: 10.1002/9781118131473.

[88] Vigneswaran S., Ngo H. H., Chaudhary D. S., Hung Y.-T. Y., Wang L. K., Hung Y.-T. Y., et al. Physicochemical treatment processes for water reuse. Physicochem. Treat. Process., 2005; 3: 635–76.

[89] Alhashimi H. A., Aktas C. B. Life cycle environmental and economic performance of biochar compared with activated carbon: A meta-analysis. Resour. Conserv. Recycl., 2017; 118: 13–26. doi: 10.1016/J.RESCONREC.2016.11.016.

[90] Sayed Jamaludin S. I., Ahmad Zaini M. A., Sadikin A. N., Abdol Jani W. N. F. Textile waste valorization as potential activated carbon precursor for the removal of water contaminants: Commentary. Mater. Today Proc., 2024; 96: 193–8. doi: 10.1016/j.matpr.2023.12.058.

[91] Li Q., Liu C., Zhao R., Tang B., Zabihi O., Naebe M. Upcycling post-consumer acrylic textiles into structural carbon fibres with reduced cost and carbon footprint. Chem. Eng. J., 2026; 531: 173853. doi: 10.1016/j.cej.2026.173853.

[92] Kadirvelu K., Thamaraiselvi K., Namasivayam C. Removal of heavy metals from industrial wastewaters by adsorption onto activated carbon prepared from an agricultural solid waste. Bioresour. Technol., 2001; 76: 63–5. doi: 10.1016/S0960-8524(00)00072-9.